

# Isospin dependence of pseudospin symmetry in nuclear resonant states

Jian You Guo<sup>1,\*</sup> and Xiang Zheng Fang<sup>1</sup>

<sup>1</sup>*School of physics and material science, Anhui university, Hefei 230039, P.R. China*

The relativistic mean field theory in combination with the analytic continuation in the coupling constant method is used to determine the energies and widths of single-particle resonant states in Sn isotopes. It is shown that there exists clear shell structure in the resonant levels as appearing in the bound levels. In particular, the isospin dependence of pseudospin symmetry is clearly shown in the resonant states, is consistent with that in the bound states, where the splittings of energies and widths between pseudospin doublets are found in correlation with the quantum numbers of single-particle states, as well as the nuclear mass number. The similar phenomenon also emerges in the spin partners.

PACS numbers: 21.10.Hw, 21.60.Jz, 25.70.Ef, 27.80.+w

## INTRODUCTION

About 30 years ago a quasi degeneracy was observed in heavy nuclei between single-nucleon doublets with quantum numbers  $(n, l, j = l+1/2)$  and  $(n-1, l+2, j = l+3/2)$  where  $n$ ,  $l$ , and  $j$  are the radial, the orbital, and the total angular momentum quantum numbers, respectively[1, 2]. The quasi-degenerative states are suggested as the pseudospin doublets  $j = \tilde{l} \pm \tilde{s}$  with the pseudo orbital angular momentum  $\tilde{l}$ , and the pseudospin angular momentum  $\tilde{s}$ , and have explained a number of phenomena in nuclear structure including deformation[3] and superdeformation[4], magnetic moment[5, 6] and identical bands[7, 8, 9]. Because of these successes, there have been comprehensive efforts to understand its origin since the discovery of this symmetry. Blokhin et al.[10] performed a helicity unitary transformation in a nonrelativistic single-particle Hamiltonian, showed that the transformed radial wave functions have a different asymptotic behavior, implying that the helicity transformed mean field acquires a more diffuse surface. Application of the helicity operator to the nonrelativistic single-particle wave function maps the normal state  $(l, s)$  onto the pseudo state  $(\tilde{l}, \tilde{s})$ , while keeping all other global symmetries. The same kind of unitary transformation was also considered earlier by Bahri et al. to discuss the pseudospin symmetry in the nonrelativistic harmonic oscillator[11]. They showed that a particular condition between the coefficients of spin-orbit and orbit-orbit terms, required to have a pseudospin symmetry in that nonrelativistic single-particle Hamiltonian, was consistent with relativistic mean-field (RMF) estimates. Based on the RMF theories, Ginocchio identifies a possible reason for this; namely that the symmetry arises from the near equality in magnitude of an attractive scalar,  $S$ , and repulsive vector,  $V$ , relativistic mean field,  $S \sim -V$ , in which the nucleons move[12]. They reveal the pseudospin symmetry is exact when doublets are degenerate. Meng et al.[13, 14] show that pseudospin symmetry is exact when  $d\Sigma/dr = 0$  where  $\Sigma = V + S$  and the quality of the pseudospin approximation in real nuclei

is connected with the competition between the pseudo-centrifugal barrier and the pseudospin-orbital potential. In other works[15, 16, 17, 18] the pseudospin symmetry has also been discussed in relation with the arguments and conjectures of Refs.[12, 13, 14]. Pseudospin symmetry has also been shown to be approximately conserved in medium energy nucleon scattering from even-even nuclei[17, 19]. A test of nuclear wave functions for pseudospin symmetry was done in Ref.[20, 21]. The structure of radial nodes occurring in pseudospin levels and a classification for the intruder levels states which do not have a pseudospin partner in the limit of pseudospin symmetry was explained as a direct effect of the behavior of nodes of Dirac bound states[22], giving support for the relativistic interpretation of nuclear pseudospin symmetry. Pseudospin symmetry is also investigated for the relativistic harmonic oscillator, and relativistic Woods-Saxon and Hulthén problem, in which the analytical solutions are obtained for the bound states of the corresponding Dirac equations by setting either  $\Sigma$  or  $\Delta (= V - S)$  to zero[23, 24, 25, 26, 27, 28]. The pseudospin breaking is shown to be connected with the mean-field shaped by the parameters of the harmonic oscillator potential[29], or the Woods-Saxon potential[30]. All these indicate the pseudospin symmetry is a good approximate for the single-particle bound states of atomic nuclei. However for the resonant states, which are thought to play a important role in formation of the exotic phenomena such as halo and skin[31, 32, 33], the symmetry has not been examined in detail for real nuclei. In recent years, many techniques have been developed to study resonant states, such as the R-matrix theory[34], the extended R-matrix theory[35], the K-matrix theory[36], S-matrix theory[37], the real stabilization method[38], the complex scaling method[39], and so on. Compared with these methods, the analytic continuation in the coupling constant (ACCC) method proposed by Kukulin[40] is more effective and numerically quite simple, has been applied to investigate the energies and widths for resonant states in the framework of the non-relativistic[41, 42, 43] and relativistic theory[44, 45]. Based on the Schrödinger and

Dirac equations, we have investigated the stability and convergence of the energies and widths for single-particle resonant states with square-well, harmonic oscillator and Woods-Saxon potentials, and discussed their dependence on the coupling constant interval and the Padé approximant (PA) order[46, 47]. Particularly, we have studied the pseudospin symmetry in the resonant states for Dirac-Woods-Saxon problem, and shown the correlations of pseudospin splittings with the shapes of Woods-Saxon mean field[48]. Considering that the RMF theory is a more microscopic one, and has gained considerable success in describing many nuclear phenomena for the stable nuclei as well as nuclei even far from stability, here we intend to study the resonant states including their pseudospin and spin symmetries by the ACCC method in the framework of RMF theory, as done for the bound states in the RMF theory[14].

## THEORETICAL FRAMEWORK

The basic ansatz of the RMF theory is a Lagrangian density whereby nucleons are described as Dirac particles which interact via the exchange of various mesons (the scalar  $\sigma$ , vector  $\omega$  and iso-vector vector  $\rho$ ) and the photon [49]

$$\begin{aligned} \mathcal{L} = & \bar{\psi}(i\cancel{\partial} - M)\psi + \frac{1}{2}\partial_\mu\sigma\partial^\mu\sigma - U(\sigma) - \frac{1}{4}\Omega_{\mu\nu}\Omega^{\mu\nu} \\ & + \frac{1}{2}m_\omega^2\omega_\mu\omega^\mu - \frac{1}{4}\mathbf{R}_{\mu\nu}\mathbf{R}^{\mu\nu} + \frac{1}{2}m_\rho^2\rho_\mu\rho^\mu - \frac{1}{4}F_{\mu\nu}F^{\mu\nu} \quad (1) \\ & - g_\sigma\bar{\psi}\sigma\psi - g_\omega\bar{\psi}\cancel{\omega}\psi - g_\rho\bar{\psi}\boldsymbol{\rho}\boldsymbol{\tau}\psi - e\bar{\psi}\mathbf{A}\psi, \end{aligned}$$

where  $M$  is the nucleon mass and  $m_\sigma$  ( $g_\sigma$ ),  $m_\omega$  ( $g_\omega$ ), and  $m_\rho$  ( $g_\rho$ ) are the masses (coupling constants) of the respective mesons. A nonlinear scalar self-interaction  $U(\sigma) = \frac{1}{2}m_\sigma^2\sigma^2 + \frac{g_2}{3}\sigma^3 + \frac{g_3}{4}\sigma^4$  of the  $\sigma$  meson has been included [50]. The field tensors for the vector mesons are given as

$$\begin{cases} \Omega^{\mu\nu} = \partial^\mu\omega^\nu - \partial^\nu\omega^\mu, \\ \mathbf{R}^{\mu\nu} = \partial^\mu\rho^\nu - \partial^\nu\rho^\mu - g^\rho(\rho^\mu \times \rho^\nu), \\ F^{\mu\nu} = \partial^\mu\mathbf{A}^\nu - \partial^\nu\mathbf{A}^\mu. \end{cases} \quad (2)$$

The classical variation principle gives the following equations of motion

$$[\boldsymbol{\alpha} \cdot \mathbf{p} + V_V(\mathbf{r}) + \beta(M + V_S(\mathbf{r}))]\psi = \varepsilon\psi, \quad (3)$$

for the nucleon spinors, where  $\varepsilon$  and  $\psi$  are the single-particle energy and spinor wave function respectively, and the Klein-Gordon equations

$$\begin{cases} (-\Delta\sigma + U'(\sigma)) = g_\sigma\rho_s, \\ (-\Delta + m_\omega^2)\omega^\mu = g_\omega j^\mu(\mathbf{r}), \\ (-\Delta + m_\rho^2)\rho^\mu = g_\rho \mathbf{j}^\mu(\mathbf{r}), \\ -\Delta A_0^\mu(\mathbf{r}) = e j_p^\mu(\mathbf{r}), \end{cases} \quad (4)$$

for the mesons, where

$$\begin{cases} V_V(\mathbf{r}) = g_\omega\psi + g_\rho\boldsymbol{\rho}\boldsymbol{\tau} + \frac{1}{2}e(1 - \tau_3)\mathbf{A}, \\ V_S(\mathbf{r}) = g_\sigma\sigma, \end{cases} \quad (5)$$

are the vector and scalar potentials respectively and the source terms for the mesons are

$$\begin{cases} \rho_s = \sum_{i=1}^A \bar{\psi}_i\psi_i, \\ j^\mu(\mathbf{r}) = \sum_{i=1}^A \bar{\psi}_i\gamma^\mu\psi_i, \\ \mathbf{j}^\mu(\mathbf{r}) = \sum_{i=1}^A \bar{\psi}_i\gamma^\mu\boldsymbol{\tau}\psi_i, \\ j_p^\mu(\mathbf{r}) = \sum_{i=1}^A \bar{\psi}_i\gamma^\mu\frac{1 - \tau_3}{2}\psi_i. \end{cases} \quad (6)$$

It should be noted that the contribution of negative energy states are neglected, i.e., the vacuum is not polarized. Moreover, the mean field approximation is carried out via replacing meson field operators in Eq. (3) by their expectation values, since the coupled equations Eq. (3) and Eq. (4) are nonlinear quantum field equations and their exact solutions are very complicated. In this way, the nucleons are assumed to move independently in the classical meson fields. The coupled equations can be solved self-consistently by iteration.

For spherical nuclei, the potential of the nucleon and the sources of meson fields depend only on the radial coordinate  $r$ . The spinor is characterized by the angular momentum quantum numbers  $l, j, m$ , the isospin  $t = \pm\frac{1}{2}$  for neutron and proton respectively. The Dirac spinor has the form

$$\psi(\mathbf{r}) = \begin{pmatrix} i\frac{G_{lj}(r)}{r}Y_{jm}^l(\theta, \phi) \\ \frac{F_{lj}(r)}{r}(\boldsymbol{\sigma} \cdot \hat{\mathbf{r}})Y_{jm}^l(\theta, \phi) \end{pmatrix} \chi_t(t), \quad (7)$$

where  $Y_{jm}^l(\theta, \phi)$  are the spinor spherical harmonics. The radial equation of the spinor, i.e. Eq. (3), can be reduced to [49]

$$\begin{aligned} \left(-\frac{\partial}{\partial r} + \frac{\kappa}{r}\right)F_{lj}(r) + [M + V_p(r)]G_{lj}(r) &= \varepsilon G_{lj}(r), \\ \left(\frac{\partial}{\partial r} + \frac{\kappa}{r}\right)G_{lj}(r) - [M - V_m(r)]F_{lj}(r) &= \varepsilon F_{lj}(r), \end{aligned} \quad (8)$$

in which  $V_p(r) = V_V(r) + V_S(r)$ ,  $V_m(r) = V_V(r) - V_S(r)$ , and  $\kappa = (-1)^{j+l+1/2}(j+1/2)$ . The meson field equations can be reduced to

$$\left(\frac{\partial^2}{\partial r^2} - \frac{2}{r}\frac{\partial}{\partial r} + m_\phi^2\right)\phi = s_\phi(r), \quad (9)$$

where  $\phi = \sigma, \omega, \rho$ , and photon ( $m_\phi = 0$  for photon).

The source terms read

$$s_\phi(r) = \begin{cases} -g_\sigma \rho_s - g_2 \sigma^2(r) - g_3 \sigma^3(r) & \text{for the } \sigma \text{ field,} \\ g_\omega \rho_v & \text{for the } \omega \text{ field,} \\ g_\rho \rho_3(r) & \text{for the } \rho \text{ field,} \\ e \rho_c(r) & \text{for the Coulomb field,} \end{cases}$$

and

$$\begin{cases} 4\pi r^2 \rho_s(r) = \sum_{i=1}^A (|G_i(r)|^2 - |F_i(r)|^2), \\ 4\pi r^2 \rho_v(r) = \sum_{i=1}^A (|G_i(r)|^2 + |F_i(r)|^2), \\ 4\pi r^2 \rho_3(r) = \sum_{p=1}^Z (|G_p(r)|^2 + |F_p(r)|^2) \\ \quad - \sum_{n=1}^N (|G_n(r)|^2 + |F_n(r)|^2), \\ 4\pi r^2 \rho_c(r) = \sum_{p=1}^Z (|G_p(r)|^2 + |F_p(r)|^2). \end{cases} \quad (11)$$

By solving Eqs. (8) and (9) in a meshed box of size  $R_0$  self-consistently, one can calculate the ground state properties of a nucleus. The vector potential  $V_V(r)$  and the scalar potential  $V_S(r)$ , energies and wave functions for bound states are also obtained. By increasing the attractive potential as  $V_p(r) \rightarrow \lambda V_p(r)$ , a resonant state will be lowered and becomes a bound state if the coupling constant  $\lambda$  is large enough. Near the branch point  $\lambda_0$ , defined by the scattering threshold  $k(\lambda_0) = 0$  [40], the wave number  $k(\lambda)$  behaves as

$$k(\lambda) \sim \begin{cases} i\sqrt{\lambda - \lambda_0}, & l > 0, \\ i(\lambda - \lambda_0), & l = 0. \end{cases} \quad (12)$$

These properties suggest an analytic continuation of the wave number  $k$  in the complex  $\lambda$  plane from the bound-state region into the resonance region by Padé approximant of the second kind (PAII) [40]

$$k(x) \approx k^{[L,N]}(x) = i \frac{c_0 + c_1 x + c_2 x^2 + \dots + c_L x^L}{1 + d_1 x + d_2 x^2 + \dots + d_N x^N}, \quad (13)$$

where  $x \equiv \sqrt{\lambda - \lambda_0}$ , and  $c_0, c_1, \dots, c_L, d_1, d_2, \dots, d_N$  are the coefficients of PA. These coefficients can be determined by a set of reference points  $x_i$  and  $k(x_i)$  obtained from the Dirac equation with  $\lambda_i > \lambda_0$ ,  $i = 1, 2, \dots, L+N+1$ . With the complex wave number  $k(\lambda = 1) = k_r + ik_i$ , the resonance energy  $E$  and the width  $\Gamma$  can be extracted from the relation  $\varepsilon = E - i\frac{\Gamma}{2}$  ( $E, \Gamma \in \mathbb{R}$ ) and  $k^2 = \varepsilon^2 - M^2$ , i.e.,

$$E = \sqrt{\frac{\sqrt{(M^2 + k_r^2 - k_i^2)^2 + 4k_r^2 k_i^2} + (M^2 + k_r^2 - k_i^2)}{2}} - M, \quad (14)$$

$$\Gamma = \sqrt{2\sqrt{(M^2 + k_r^2 - k_i^2)^2 + 4k_r^2 k_i^2} - 2(M^2 + k_r^2 - k_i^2)}.$$

In the non-relativistic limit ( $k \ll M$ ), Eq. (14) reduces to

$$E = \frac{k_r^2 - k_i^2}{2M}, \quad \Gamma = \frac{2k_r k_i}{M}. \quad (15)$$

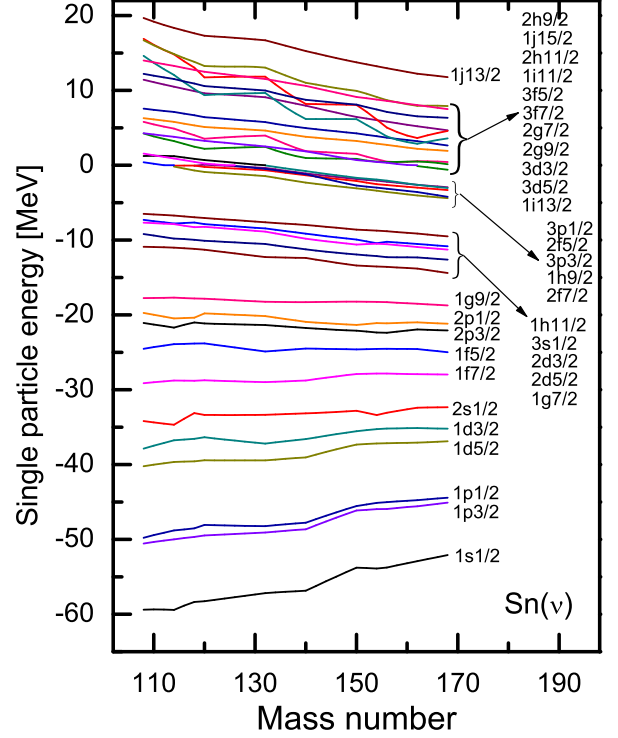


Fig. 1: The single-particle energies of neutron as the function of mass number for Sn isotopes, where the energies of resonant states obtained by the ACCC method in the RMF theory with the interactions NL3.

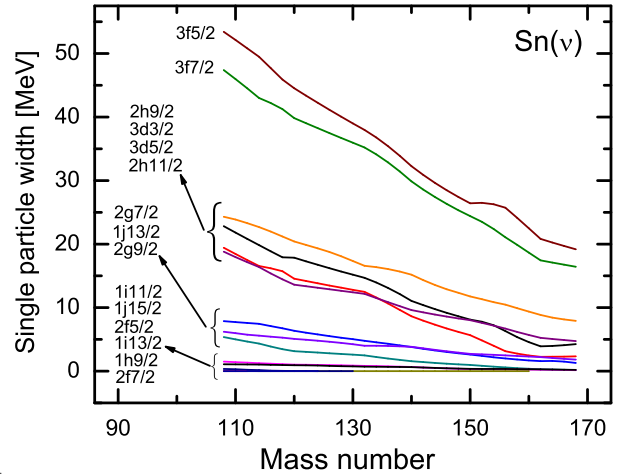


Fig. 2: The same as Fig.1, but for the single-particle widths of neutron.

## NUMERICAL DETAILS AND RESULTS

With the technique represented above, we first single out the resonant states in the continuum for Sn isotopes, and then analyze their properties including the pseudospin and spin symmetries. Following Refs.[45, 46, 47, 48], the radial Dirac equations (8) are solved in a standard way by the shooting method with a step size of 0.05 fm using proper boundary conditions in a spherical box of radius  $R = 20$  fm[49]. The branch point  $\lambda_0$  is determined in a self-consistent way as in Ref.[40]. In correspondence to  $L + N + 1$  different coupling constant values  $\lambda_i > \lambda_0$ , we solve the bound state problem for  $\lambda_i \Sigma(r)$ , and obtain the eigenvalues  $\varepsilon_i$  from the Dirac equations. The solutions of the linear equations are the coefficients in the PA expression (13). With the coefficients in Eq.(13), the wave number as a function of the coupling constant  $k(\lambda)$  can be obtained. Then the energy and width of a resonant state can be extracted from the complex wave number  $k(\lambda = 1)$ . Considering that there are a little influences of the coupling constant interval and the Padé approximant order on the calculated results in the ACCC method as shown in Ref.[48], we first check the stability and convergence of this method in the present framework to choose reasonably the coupling constant interval and the Padé approximant order for Sn isotopes. Similar to the Figs.2 and 3 in Ref.[48], the energies and widths of resonant states are found to be considerable stable in a fairly large coupling constant interval for fixed order, especially for the calculations with (5,5) PAs. Based on the fact, all the energies and widths for resonant states in the following are taken from the calculations of (5,5) PA with  $\lambda_b - \lambda_0 = 1$  as done in Ref.[48], in which the branch point  $\lambda_0$  and  $\lambda_b$  are respectively the left and right edge of the coupling constant interval in the Padé approximant.

To see the behavior of the single-particle resonant states and their isospin dependence as well as comparison with the case of bound states, the energy as a function of the mass number are displayed in Fig.1 for the Sn isotopes. Except for several small kinks, the energies are shown to decrease monotonously with the increasing isospin for all the resonant states, which is in agreement with that for the bound states near the threshold, different from that for the bound states far from the threshold where the change is altered with a contrary trend as the level  $1s_{1/2}$ . For the resonant states  $3d_{3/2}, 3d_{5/2}, 3f_{5/2}$ , and  $3f_{7/2}$ , the energies decrease more quickly, and happen to cross with their neighbor at several Sn nuclei, which does not appear in the bound states. Particularly, there are several kinks in these levels as appearing in the bound levels at a less extent, e.g.: the  $1s_{1/2}, 2s_{1/2}, 2p_{1/2}$ , and  $2p_{3/2}$ . These kinks always appear at several special positions for whether the bound or resonant states, may reflect some special structure existing in these nuclei. Besides of the kinks, several large gaps are found in

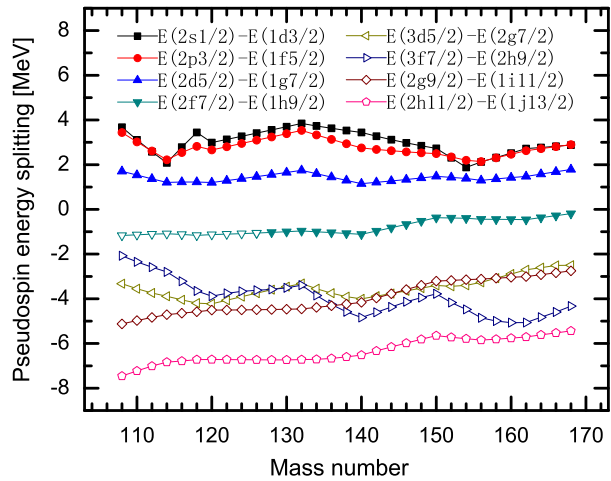


Fig. 3: The energy splittings of pseudospin doublets as the function of mass number for Sn isotopes, where the filled and opened marks represent respectively for bound and resonant states.

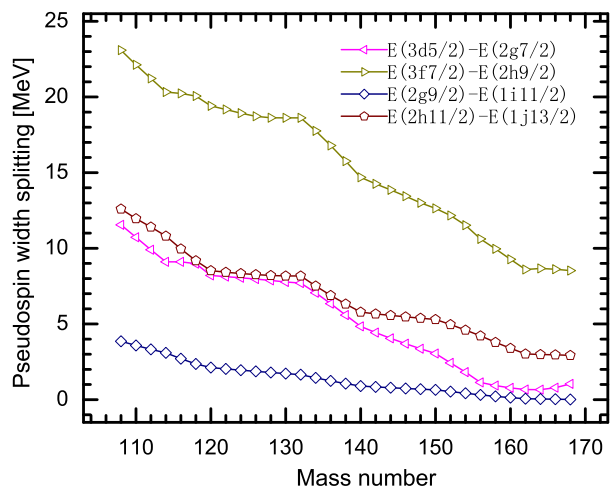


Fig. 4: The same as Fig.3, but for the width splittings of pseudospin doublets for Sn isotopes.

the resonant levels as appearing in the bound levels. The large energy gap between the levels  $2f_{7/2}$  and  $1h_{11/2}$  remain hardly change whether these levels are unbound or lowered to bound. The same phenomenon also appear in the resonant levels between  $1j_{13/2}$  and  $2h_{9/2}$ . From these phenomena we see that the resonant levels also provide the detailed information on nuclear shell structure.

Compared with the energies, the widths of the resonant states also decrease monotonously with the increasing isospin, which can be seen in Fig.2. Especially for the resonant states  $3d_{3/2}, 3d_{5/2}, 3f_{5/2}$ , and  $3f_{7/2}$ , the behavior of decreasing more quickly, even crossing with their neighbor in the energies also appears in the widths. Moreover, the shell structure is clearly shown with several large gaps in the widths for several different reso-

nant states. The large energy gap between  $2h_{9/2}$  and  $3f_{7/2}$  decreases with the increasing isospin. The same phenomenon also appears between the levels  $1i_{11/2}$  and  $2g_{9/2}$ . In comparison with the energies, the widths decrease in general more quickly, especially for the  $3f_{5/2}$  and  $3f_{7/2}$ .

With these knowledge on the energies and widths, we analyze the symmetry existing in these resonant states. As identified to be a good approximation in the bound states, the pseudospin symmetry worths being examined for the single-particle resonant states. In Ref.[48], the symmetry in the resonant states has been investigated by solving the Dirac equation with Woods-Saxon potentials in combination with the ACCC method, where the pseudospin breaking is shown in correlation with the shapes of nuclear mean-field. In order to examine the symmetry in the framework of RMF theory, and study their isospin dependence, which has been discussed in the bound states[14], we analyze the relation between the pseudospin splitting and the nuclear mass number for the resonant states. The dependence is shown in Fig.3 for the Sn isotopes, where the energy splittings of bound states are also exhibited for comparison. From Fig.3, it can be seen that the pseudospin symmetry in the resonant states is correlated with the quantum numbers of single-particle states, and the pseudospin splittings are different from the different pseudospin partners, which is in agreement with the case of bound states[30] as well as the case of resonant states in Dirac Woods-Saxon mean field approximation[48]. As far as the isospin dependence of the pseudospin orbital splitting is concerned, the splittings between the resonant doublets give a monotonous decreasing behavior with the increasing isospin with only the  $3f_{7/3}$  and  $2h_{9/2}$  partner exception. Particularly for the  $2g_{9/2}$  and  $1i_{11/2}$  partner, the pseudospin splitting in  $^{168}\text{Sn}$  is only half of that in  $^{108}\text{Sn}$ . Just as we expected, the pseudospin symmetry in neutron-rich nuclei is better, which agrees the case of the bound levels. Besides of the isospin dependence, the pseudospin splitting is also correlated with the radial, orbital, and total angular momentum quantum numbers. Such as the splitting between the  $2h_{11/2}$  and  $1j_{13/2}$  partner is 2 MeV larger than that between the  $2g_{9/2}$  and  $1i_{11/2}$  partner. In comparison with the resonant states, the situation in the bound pseudospin partners is more complicated, but the pattern is more or less the same, i.e., a decreasing behavior with the increasing isospin with some exceptions. For example, the splittings between the levels  $2s_{1/2}$  and  $1d_{3/2}$ , and between the levels  $2p_{3/2}$  and  $1f_{5/2}$  show a decreasing trend in a complicated way, while that  $2d_{5/2}$  and  $1g_{7/2}$  presents a minor variation in the whole Sn isotope chain. It should be mentioned for the  $2f_{7/2}$  and  $1h_{9/2}$  partner, the same trend for the change of pseudospin splitting is seen whether they are bound or evolved to unbound states. For all the pseudospin partners with the same radial quantum number, the energy splitting is dis-

covered to evolve from  $E_{n,l,j=l+1/2} > E_{n-1,l+2,j=l+3/2}$  to  $E_{n,l,j=l+1/2} < E_{n-1,l+2,j=l+3/2}$  with the increasing orbital angular momentum. This inversion of pseudospin splittings is observed experimentally, was found in Refs.[14, 15, 51, 52] in the bound states, also appears in the resonant states here.

For width (to see Fig.4), similar to the energy, the pseudospin splittings decrease monotonously with the increasing mass number with no exception. The widths for all the single particle states with quantum numbers  $(n,l,j = l + 1/2)$  are systemically larger than that of their pseudospin partners  $(n - 1, l + 2, j = l + 3/2)$ , which implies that the resonant states with higher orbital angular momentum hold longer decay time than their pseudospin partners. It is because that the orbital angular momentum is smaller, the centrifugal barrier is lower, the resonant width is larger. Hence, even the energy is fully degenerate for the pseudospin doublet, their decay life maybe still different, which is noticeable to explore the resonant state from experiment. From these studies, we see that the pseudospin symmetry remains a good approximation for both stable and exotic nuclei. A better pseudospin symmetry can be expected for the orbital near the threshold, particularly for nuclei near the particle drip line.

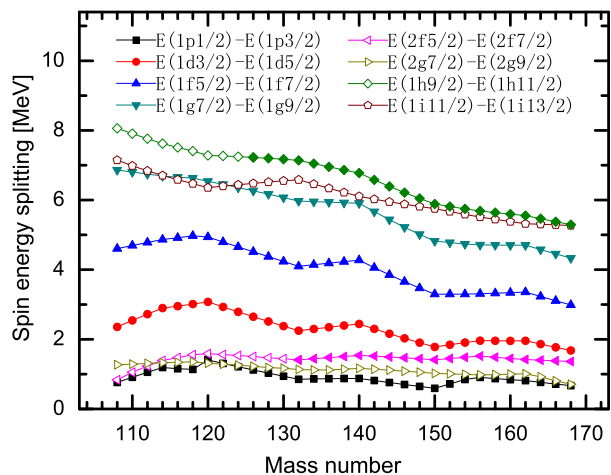


Fig. 5: The energy splittings of spin doublets as the function of mass number for Sn isotopes, where the filled and opened marks represent respectively to the cases of bound and resonant states.

In order to compare with the pseudospin symmetry, the spin orbital splittings as a function of the mass number are plotted in Fig.5 for the Sn isotopes, where a more distinct decreasing behavior with the increasing mass number is clearly seen for both the bound and unbound spin partners with few exceptions. It shows that the spin symmetry in neutron-rich nuclei is also better such as the pseudospin symmetry. In addition, the spin orbital splitting is also correlated with the quan-

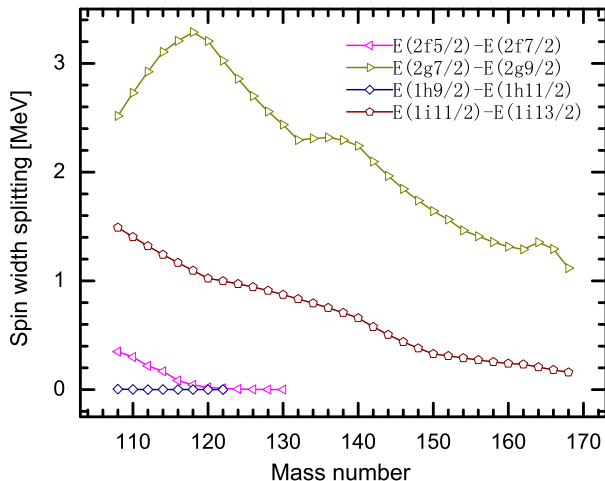


Fig. 6: The same as Fig.5, but for the width splittings of spin doublets for Sn isotopes.

tum numbers of single-particle states. For the spin doublets with the same radial quantum number, the energy splitting increases with the increasing orbital angular momentum for the bound states, which is contrary to the resonant states. Compared with pseudospin symmetry, the inversion of spin splitting has not been found for whether the bound or unbound spin partners. The energies for the single particle states with quantum numbers  $(n, l, j = l - 1/2)$  are systematically larger than that of their spin partners  $(n, l, j = l + 1/2)$ , which indicates that the single-particle states with higher total angular momentum are more stable than their spin partners. It agrees the experimental facts as observed in the nuclear bound states. For the width, similar to the pseudospin symmetry, a monotonous decreasing behavior with the increasing isospin is seen in Fig.6 with a bit special in several nuclei. The widths for the single particle states with quantum numbers  $(n, l, j = l - 1/2)$  are systematically larger than that of their spin partners  $(n, l, j = l + 1/2)$ , which implies that the resonant states with higher total angular momentum hold longer decay time than their spin partners, is similar to the case of pseudospin symmetry. From these results we see that the spin orbital splitting is also very sensitive to the quantum numbers of single-particle states. The spin symmetry remains a better approximation for the bound states with lower orbital angular momentum, while for resonant states with higher orbital angular momentum, particularly for nuclei near the particle drip line.

## CONCLUSION

The relativistic mean field theory in combination with the analytic continuation in the coupling constant method is adopted to determine the energies and widths

of single-particle resonant states for the Sn isotopes, where the energies are found to decrease monotonously with the increasing isospin with several small kinks, is in agreement with the case of bound states near the threshold. In addition, the shell structure is seen clearly in the resonant levels with several large gaps as appearing in the bound levels. In particular, the pseudospin and spin symmetries in the resonant states are investigated and compared with that in the bound states, where the symmetries are found to be correlated with the quantum numbers of single-particle states, which is similar to the case of bound states. As far as the isospin dependence is concerned, the pseudospin and spin splittings between the resonant doublets give a monotonous decreasing behavior with the increasing isospin with few exceptions. The same phenomenon also appear between the bound doublets. The trend of energy splittings with the orbital angular momentum is found to be consistent with the case of bound for all the pseudospin partners, which is not consistent with the spin partners. The inversion of energy-splitting appears in several pseudospin partners of resonant states, which agrees with the experimental observation, as well as the case of bound states and the nonrelativistic prediction, while the inversion does not appear in the spin doublets. The tendency of width splittings with the parameters is displayed to be agreeable for all the pseudospin partners, as well as the spin partners. The widths for the single particle states with higher orbital (total) angular momentum are systematically larger than that of their pseudospin (spin) partners, which show that even the fully degenerate pseudospin (spin) doublets may exist different decay time, making them worthy of experimental attention.

This work was partly supported by the National Natural Science Foundation of China under Grant No. 10475001, the Program for New Century Excellent Talents in University of China, and the Excellent Talents Foundation in University of Anhui Province in China.

\* Electronic address: jianyou@ahu.edu.cn

- [1] K.T. Hecht and A. Adler, Nucl. Phys. **A137**, 129 (1969).
- [2] A. Arima, M. Harvey, and K. Shimizu, Phys. Lett. **30B**, 517 (1969).
- [3] A. Bohr, I. Hamamoto, and B.R. Mottelson, Phys. Scr. **26**, 267 (1982).
- [4] J. Dudek, W. Nazarewicz, Z. Szymanski and G.A. Leander, Phys. Rev. Lett. **59**, 1405 (1987).
- [5] D. Troltenier, W. Nazarewicz, Z. Szymanski, and J.P. Draayer, Nucl. Phys. **A567**, 591 (1994).
- [6] A.E. Stuchbery, J. Phys. **G25**, 611 (1999); A.E. Stuchbery, Nucl. Phys. **A700**, 83 (2002).
- [7] W. Nazarewicz, P.J. Twin, P. Fallon and J.D. Garrett, Phys. Rev. Lett. **64**, 1654 (1990).
- [8] F.S. Stephens, M. A. Deleplanque, and J. E. Draper et al., Phys. Rev. Lett. **65**, 301 (1990); F.S. Stephens, M.

- A. Deleplanque, and A. O. Macchiavelli et al., Phys. Rev. **C57**, R1565 (1998).
- [9] J.Y. Zeng, J. Meng, C.S. Wu, E.G. Zhao, Z. Xing and X.Q. Chen, Phys. Rev. **C44**, R1745 (1991).
- [10] A.L. Blokhin, C. Bahri, and J.P. Draayer, Phys. Rev. Lett. **74**, 4149 (1995).
- [11] C. Bahri, J.P. Draayer, and S.A. Moszkowski, Phys. Rev. Lett. **68**, 2133 (1992).
- [12] J.N. Ginocchio, Phys. Rev. Lett. **78**, 436 (1997); Phys. Rep. **315**, 231 (1999).
- [13] J. Meng, K. Sugawara-Tanabe, S. Yamaji, P. Ring, and A. Arima, Phys. Rev. **C58**, R628 (1998).
- [14] J. Meng, K. Sugawara-Tanabe, S. Yamaji, and A. Arima, Phys. Rev. **C59**, 154 (1999).
- [15] G.A. Lalazissis, Y.K. Gambhir, J.P. Maharana, C.S. Warke, and P. Ring, Phys. Rev. **C58**, R45 (1998).
- [16] J.N. Ginocchio and D.G. Madland, Phys. Rev. **C57**, 1167 (1998).
- [17] J.N. Ginocchio, Phys. Rev. Lett. **82**, 4599 (1999).
- [18] K. Sugawara-Tanabe and A. Arima, Phys. Rev. **C58**, R3065 (1998).
- [19] H. Leeb and S. Wilmsen, Phys. Rev. **C62**, 024602 (2000).
- [20] J.N. Ginocchio and A. Leviatan, Phys. Rev. Lett. **87**, 072502 (2001).
- [21] J.N. Ginocchio, Phys. Rev. **C66**, 064312 (2002).
- [22] A. Leviatan and J.N. Ginocchio, Phys. Lett. **B518**, 214 (2001).
- [23] T.S. Chen, H.F. Lü, J. Meng, S.Q. Zhang, and S.G. Zhou, Chin. Phys. Lett. **20**, 358 (2003).
- [24] J.N. Ginocchio, Phys. Rev. **C69**, 034318 (2004).
- [25] R. Lisboa and M. Malheiro, A.S. de Castro, P. Alberto, and M. Fiolhais, Phys. Rev. **C69**, 024319 (2004).
- [26] J.Y. Guo, X.Z. Fang, and F.X. Xu, Phys. Rev. **A66**, 062105 (2002).
- [27] J.Y. Guo, Z.Q. Sheng, Phys. Lett. **A338**, 90 (2005).
- [28] J.Y. Guo, J. Meng, and F.X. Xu, Chin. Phys. Lett. **20**, 602 (2003).
- [29] J.Y. Guo, X.Z. Fang, and F.X. Xu, Nucl. Phys. **A757**, 411 (2005).
- [30] P. Alberto, M. Fiolhais, M. Malheiro, A. Delfino, and M. Chiapparini, Phys. Rev. Lett. **86**, 5015 (2001); Phys. Rev. **C65**, 034307 (2002).
- [31] J. Meng and P. Ring, Phys. Rev. Lett. **77**, 3963 (1996); Phys. Rev. Lett. **80**, 460 (1998).
- [32] N. Sandulescu, L.S. Geng, H. Toki, and G.C.Hillhouse, Phys. Rev. **C68**, 054323 (2003).
- [33] L.G. Cao and Z.Y. Ma, Phys. Rev. **C66**, 024311 (2002).
- [34] E. Wigner and L. Eisenbud, Phys. Rev. **72**, 29 (1947).
- [35] G.M. Hale, R.E. Brown, and N. Jarmie, Phys. Rev. Lett. **59**, 763 (1987).
- [36] J. Humblet, B.W. Filippone, and S.E. Koonin, Phys. Rev. **C44**, 2530 (1991).
- [37] J.R. Taylor, *Scattering Theory: The Quantum Theory on Nonrelativistic Collisions*, (John Wiley & Sons, New York, 1972).
- [38] A.U. Hazi and H.S. Taylor, Phys. Rev. **A1**, 1109 (1970).
- [39] Y.K. Ho, Phys. Rep. **99**, 1 (1983).
- [40] V.I. Kukulin, V.M. Krasnopl'sky and J. Horáček, *Theory of Resonances: Principles and Applications* (Kluwer Academic, Dordrecht, 1989).
- [41] N. Tanaka, Y. Suzuki, and K. Varga et al. Phys. Rev. **C59**, 1391 (1999).
- [42] S. Aoyama, Phys. Rev. Lett. **89**, 052501 (2002).
- [43] G. Cattapan and E. Maglione, Phys. Rev. **C61**, 067301 (2000).
- [44] S.C. Yang, J. Meng, and S.G. Zhou, Chin. Phys. Lett. **18**, 196 (2001).
- [45] S.S. Zhang, J. Meng, S.G. Zhou, and G.C. Hillhouse, Phys. Rev. **C70**, 034308 (2004).
- [46] S.S. Zhang, J. Meng, and J.Y. Guo, High Ener. Phys. and Nucl. Phys. **27**, 1095 (2003) (in Chinese).
- [47] S.S. Zhang, J.Y. Guo, S.Q. Zhang, and J. Meng, Chin. Phys. Lett. **21**, 632 (2004).
- [48] J.Y. Guo, R.D. Wang, and X.Z. Fang, Phys. Rev. **C72**, 054319 (2005).
- [49] J. Meng, Nucl. Phys. **A635**, 3 (1998).
- [50] J. Boguta and A. R. Bodmer, Nucl. Phys. **A292**, 413(1977).
- [51] S. Marcos, L.N. Savushkin, M. López-Quelle, and P. Ring, Phys. Rev. **C62**, 054309 (2000).
- [52] S. Marcos, M. López-Quelle, R. Niembro, L.N. Savushkin, and P. Bernardos, Phys. Lett. **B513**, 30 (2001).